J|A|C|S COMMUNICATIONS

Published on Web 12/04/2008

Structure of Isolated Biomolecules by Electron Diffraction−Laser Desorption: Uracil and Guanine

Andreas Gahlmann, Sang Tae Park, and Ahmed H. Zewail*

Physical Biology Center for Ultrafast Science and Technology, Arthur Amos Noyes Laboratory of Chemical Physics, California Institute of Technology, Pasadena, California 91125

Received November 6, 2008; E-mail: zewail@caltech.edu

Ultrafast electron diffraction (UED) has been developed to study structural dynamics in isolated molecules in the gas phase with combined spatial and temporal resolutions.[1−3] The power of diffraction is in the ability to determine structures and, when time-resolved, provide those of excited states and dark structures.[4] However, all forms of gas-phase electron diffraction (GED)[5] have been limited to molecular specimens, which develop an appreciable vapor pressure upon thermal heating. With conventional heating, GED studies of uracil,[6] cytosine,[7] and thymine[8] have been reported, and for all, transitional heating (below the decomposition threshold) had to be controlled. In general, large molecules, and in particular those of biological importance, tend to undergo thermal reactions and degradation, making them out of reach for structural and dynamic studies.

Given this limitation with respect to large biomolecules, it is of great value to develop an alternate methodology to deliver these systems into the gas phase in sufficient density, such that their structure as well as their intrinsic structural dynamics can be investigated with UED in the absence of a perturbing solvent. However, it is essential to achieve high density and sensitivity. In GED experiments, the typical average current is microampere (6×10^{12} e/s), orders of magnitude larger than the current generated in UED-3, picoampere (2×10^{7} e/s). Thus to perform any successful UED experiment, given the difference in electron count, the molecular density has to be significantly higher, by at least 4 orders of magnitude, in the interaction region. With heating, such a density of molecules will not be reached without decomposition.

In this contribution, we report the first successful electron diffraction of biomolecules achieved with surface-assisted infrared laser desorption. The capability of this method in the newly constructed fourth generation electron diffraction apparatus (UED-4) is demonstrated by determining the structures of the RNA nucleobase, uracil, and the DNA nucleobase, guanine. The density is estimated to be higher than needed, reaching $\sim 10^{15}$ molecules/cm^3, and the sensitivity is sufficient to determine the structures. The refined structures are compared to those obtained using density functional theory.

When interfacing the UED apparatus with a laser desorption system, it is critical that the vapor plume contains only the species of interest in its monomeric form, because the probing electron pulse does not discriminate between the different chemical species it interacts with. Any significant fragmentation or cluster formation of the sample would make the analysis of the resulting diffraction pattern complex. Surface-assisted laser desorption in the absence of matrix molecules or particles, but utilizing a strongly absorbing immobilized substrate,[9] avoids the presence of a chemical background in the vapor plume. Furthermore, because the molecular sample is largely transparent to the infrared (IR) light, the energy deposited into the internal degrees of freedom of the molecule is limited by the extent of energy transfer between the sample and the surface.[10,11] In fact, in mass spectrometry, with relatively low molecular densities ($\sim 10^{6}$ molecules/shot),[12] far below what is needed here, surface-assisted laser desorption has been employed to vaporize polypeptides containing as many as 10 amino acids without significant degradation,[13] but most desorption studies have been made using matrices to deliver massive biomolecules into the gas phase in low density.[12,14]

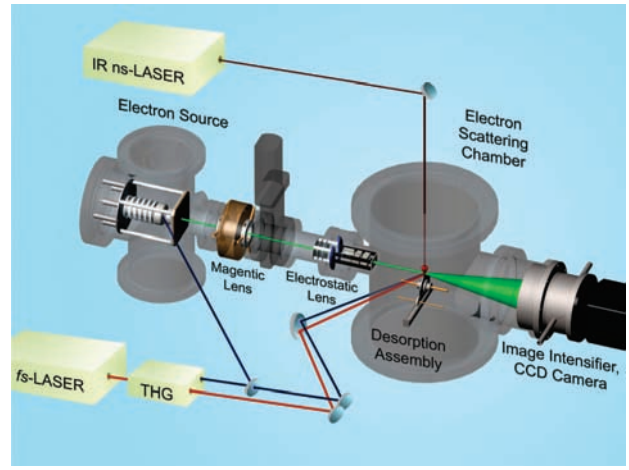

Figure 1. Schematic illustration of the electron diffraction-laser desorption (UED-4) apparatus. We note that, besides the two fs lasers used in UED studies,[1−4] here, an additional third laser is used to desorb the molecules into the gas phase. See text for details.

The experimental setup of the UED-4 apparatus is shown in a schematic representation in Figure 1, which highlights the newly designed sample-delivery assembly and the electron-pulse generation source. Briefly, two wheels in contact with each other, a felt brush wheel and a glassy carbon substrate wheel, were positioned inside a "scoop" with the brush wheel adjacent to the sample. The fine powder of uracil or guanine (Aldrich) was filled into this rectangular scoop and mounted inside the scattering chamber. During the experiment, the scoop and the sample within were slowly translated, by a precision mechanical stage, toward the brush wheel, which then transferred small amounts of the powder onto the surface of the substrate wheel. The two wheels were rotated in the same direction to ensure that, through friction, a thin and uniform film of sample was continuously applied onto the substrate surface. A cylindrically focused IR laser (1064 nm, <2 ns pulse width, <200 mJ/cm^2) was used to desorb the sample from the substrate. Because a single pulse of the desorption laser vaporized all the sample within its footprint (see Figure 2a), the substrate wheel was rotated at 80 rpm to ensure that a freshly covered surface was exposed to every laser pulse at a repetition rate of 1 kHz.

The gas plume was intersected by a pulsed electron beam (700 μm full width at half-maximum, 200 000 electrons/pulse) at a

10.1021/ja808720j CCC: $40.75

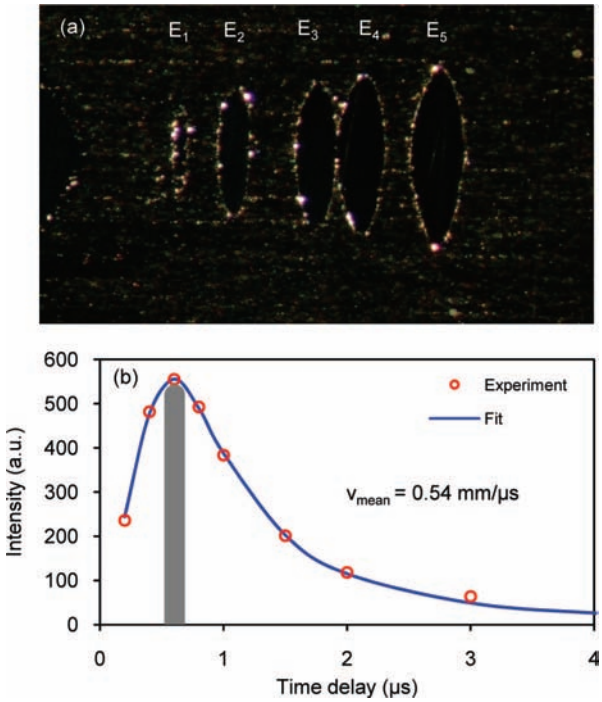

Figure 2. Image and intensity of the plume. (a) Image of the substrate after single shots of IR laser at different pulse energies: $E_1 = 90\ \mu J$, $E_2 = 170\ \mu J$, $E_3 = 260\ \mu J$, $E_4 = 340\ \mu J$, $E_5 = 420\ \mu J$. (b) Scattering intensity as a function of the time delay between the desorption laser and the electron pulse.

distance of 750 μm from the substrate surface. The electron pulses were generated by front illumination of a magnesium target using an attenuated femtosecond ultraviolet (UV) laser (267 nm, 120 fs pulse width), accelerated to 60 keV, focused by a magnetic lens, and steered by electrostatic deflection. Temporal synchronization between the desorption IR laser pulses and the electron generating UV laser pulses was made using a digital delay generator. Diffraction patterns were recorded on an image intensifier-CCD camera and analyzed using home-built software. The stability of the plume is evident in the current ability to record diffraction for 13 h. However, the machine is designed to operate continuously for several days, if needed. For structural refinement, starting geometries and vibrational force constants were obtained at the B3LYP/6−311G(d,p) level of theory using the Gaussian 98 software package.[15]

From the temporal and the spatial alignment between surface-desorbed molecules and the electron pulse, we can obtain the translational profile of the plume. Figure 2b gives the recorded scattering as a function of the delay time between the electron and the IR pulses. The scattering signal is maximum at a delay time of 0.6 μs and when the electron pulse probes the plume 750 μm above the surface. Using a simple model with a shifted Gaussian distribution of *initial* velocity, we obtained a translational temperature of ~4900 K and a mean velocity of ~0.54 mm/μs.[16] The mean velocity value is larger than the speed of sound, being in the supersonic regime of plume expansion.[17]

In Figure 3, we depict the electron diffraction obtained for uracil using the surface-desorption method. Shown are the molecular scattering function, $sM(s)$, and the radial distribution, $f(r)$. From them, we determined the molecular structure; the methodology is described elsewhere.[2] Uracil, one of the RNA bases, can exist in four different tautomers. Quantum chemical calculations predict that the diketo form is more stable than enol forms by at least 10 kcal/mol.[18] The calculations were substantiated by spectroscopic

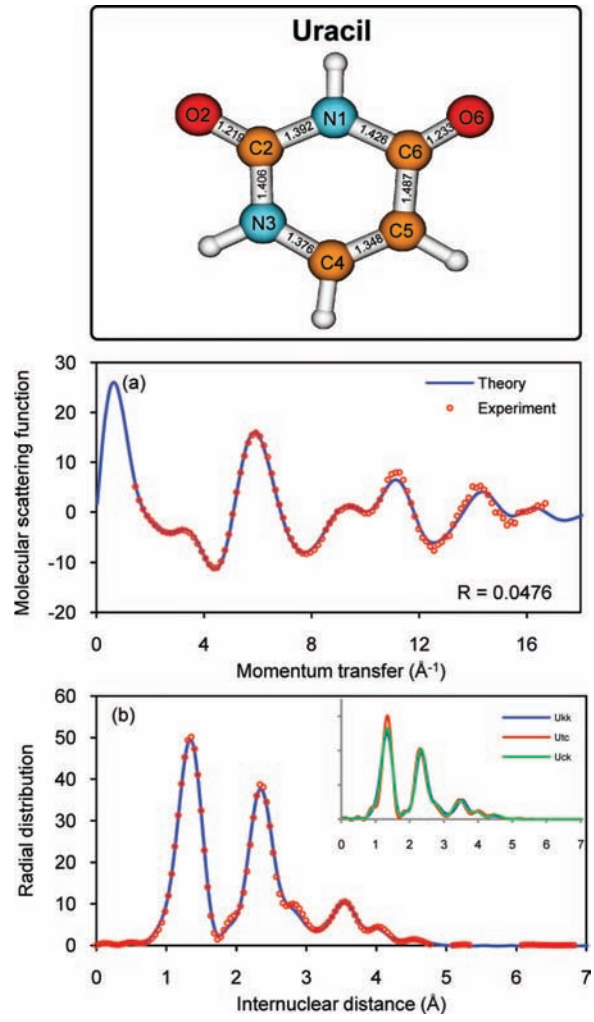

Figure 3. Diffraction of uracil. Shown are (a) the molecular scattering function, $sM(s)$, and (b) the radial distribution, $f(r)$, for the experimental (points) and theoretical (line) curves, together with theoretical results for the different tautomers. Also shown are the molecular structure of uracil and the atomic designations. As in a previous study,[1] the number of independent structural parameters included in the refinement was chosen, such that the experimental noise did not affect the determined bond lengths and angles beyond the well-known chemical structural information of, e.g., C−C bonds, *etc.*; four parameters were used to refine the structure of uracil.

studies that only detected the diketo form.[18,19] Dimers and clusters can also form,[20] but they are less favorable at high temperature and low pressure conditions. Here, we considered both the lowest- and higher-energy tautomers for the recorded diffraction, using DFT calculations of the structures.

The experimental and theoretical (modified) molecular scattering functions in Figure 3a show good agreement, with the quality of fit, R, of 0.0476, which is near the optimum value $R = 0$. The observed $sM(s)$ and $f(r)$ were analyzed and refined for the most stable diketo tautomer. A vibrational temperature of 1400 K was deduced from the best fit to the experimental diffraction pattern, which is less than the measured translational temperature (an incomplete energy exchange), explaining the abundance of intact molecular species on the μs time scale. It is to be noted that uracil is planar, even though it is not aromatic; conjugation of the C═O and C═C double bonds is reflected in the change of bond lengths shown in Figure 3.

Guanine, which is a base for both RNA and DNA, was the second molecular structure we studied. Many isomers can exist due

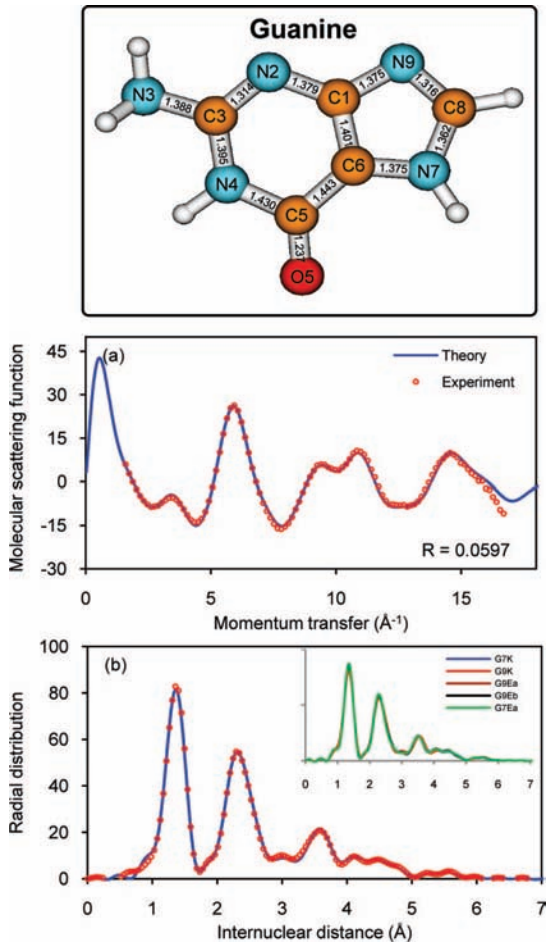

Figure 4. Diffraction of guanine. Shown are (a) the molecular scattering function, $sM(s)$, and (b) the radial distribution, $f(r)$, for the experimental (points) and theoretical (line) curves, together with theoretical results for the different tautomers. Also shown are the molecular structure of guanine and the atomic designations. Two independent parameters were used to refine the structure of guanine (see Figure 3).

to tautomerism as well as the possible hydrogen presence on nitrogen atoms.[21] However, the keto forms are lowest in energy,[22] and the four most stable isomers were identified in a helium nanodroplet study.[23] Figure 4 depicts the diffraction data of guanine, which were analyzed for the G7K isomer, one of the stable keto forms. The electron diffraction patterns of the G9K form, which only differs by the hydrogen position, is very similar to the assumed G7K isomer and almost indistinguishable within our current sensitivity (see Figure 4b inset); thus, their relative fractions cannot be determined reliably at this stage. Experimental and theoretical modified molecular scattering functions in Figure 4a show satisfactory agreement, with the quality of fit, R, of 0.0597, despite the one-tautomer assumption made. A vibrational temperature of 1600 K was deduced, again, based on the best fit of the diffraction pattern. Guanine is also a conjugated system; the single bonds are shorter than typical single-bond lengths, indicating that aromaticity is not totally lost.

Given the success of the electron diffraction-laser desorption studies reported here, UED-4 is now poised to explore other isolated large biomolecules, including polypeptides and possibly functional proteins. Naturally, the focus will be on overall conformation changes and motifs, with manifested nonbonded higher-order nearest neighbor distances, rather than the structural details contained in direct bond distances. In a recent theoretical account, it has been demonstrated that it should be possible to observe helix-to-coil transitions in gaseous polypeptides and proteins,[24,25] an area we are currently pursuing with UED-4. As with other UED studies, introducing an initial (clocking) pulse, Figure 1, will enable the study of structural dynamics to follow the molecular rearrangements in real time, from the ps to the μs regime.

Acknowledgment. This research was supported by the Air Force Office of Scientific Research and the Gordon and Betty Moore Foundation. We would like to thank Professor Samuel Leutwyler and his group for providing the theoretical geometries of the hydrogen bonded uracil dimers and I-Ren Lee for his help and discussion.

References

(1) Park, S. T.; Gahlmann, A.; Zewail, A. H. *Angew. Chem., Int. Ed.* **2008**, *47*, 9496–9499.
(2) Park, S. T.; Feenstra, J. S.; Zewail, A. H. *J. Chem. Phys.* **2006**, *124*, 174707.
(3) Srinivasan, R.; Lobastov, V. A.; Ruan, C.-Y.; Zewail, A. H. *Helv. Chim. Acta* **2003**, *86*, 1763–1838. and references therein. .
(4) Srinivasan, R.; Feenstra, J. S.; Park, S. T.; Xu, S. J.; Zewail, A. H. *Science* **2005**, *307*, 558–563.
(5) Hargittai, I.; Hargittai, M. *Stereochemical Applications of Gas-Phase Electron Diffraction*; VCH Publishers, Inc: New York, 1988.
(6) Ferenczy, G.; Harsányi, L.; Rozsondai, B.; Hargittai, I. *J. Mol. Struct.* **1986**, *140*, 71–77.
(7) Shorokhov, D. Ph.D. Dissertation, University of Oslo, 2000.
(8) Vogt, N.; Khaikin, L. S.; Grikina, O. E.; Rykov, A. N.; Vogt, J. *J. Phys. Chem. A* **2008**, *112*, 7662–7670.
(9) Pajasová, L.; Soukup, L.; Jastrabík, L.; Chvostová, D. *Surf. Rev. Lett.* **2002**, *9*, 473–477.
(10) Handschuh, M.; Nettesheim, S.; Zenobi, R. *J. Phys. Chem. B* **1999**, *103*, 1719–1726.
(11) Maechling, C. R.; Clemett, S. J.; Engelke, F.; Zare, R. N. *J. Chem. Phys.* **1996**, *104*, 8768–8776.
(12) Dreisewerd, K. *Chem. Rev.* **2003**, *103*, 395–425.
(13) Speir, J. P.; Amster, I. *J. Anal. Chem.* **1992**, *64*, 1041–1045.
(14) Levis, R. J. *Annu. Rev. Phys. Chem.* **1994**, *45*, 483–518.
(15) Frisch, M. J., et al.; Gaussian Inc.: Pittsburgh, PA, 1998.
(16) From the known fluences and heat capacities, the estimated temperature is found to be in the range calculated by thermodynamic consideration. After laser absorption, the temperature of the substrate is estimated to be ~6000 K and for solid uracil (different heat capacity and mass) an upper value of ~5800 K will be reached, if all energy is exchanged. We note that the melting temperature of uracil is 608 K, but the system, on such short time scales, transfers into the gas phase at the low pressure of the chamber (10^{-6} torr).
(17) Kelly, R.; Dreyfus, R. W. *Surf. Sci.* **1988**, *198*, 263–276.
(18) Vaquero, V.; Sanz, M. E.; López, J. C.; Alonso, J. L. *J. Phys. Chem. A* **2007**, *111*, 3443–3445.
(19) Choi, M. Y.; Miller, R. E. *J. Phys. Chem. A* **2007**, *111*, 2475–2479.
(20) Pitoňák, M.; Riley, K. E.; Neogrády, P.; Hobza, P. *ChemPhysChem* **2008**, *9*, 1636–1644.
(21) Ha, T.-K.; Keller, H.-J.; Gunde, R.; Gunthard, H.-H. *J. Phys. Chem. A* **1999**, *103*, 6612–6623.
(22) Hanus, M.; Ryjáček, F.; Kabeláč, M.; Kubař, T.; Bogdan, T. V.; Trygubenko, S. A.; Hobza, P. *J. Am. Chem. Soc.* **2003**, *125*, 7678–7688.
(23) Choi, M. Y.; Miller, R. E. *J. Am. Chem. Soc.* **2006**, *128*, 7320–7328.
(24) Lin, M. M.; Shorokhov, D.; Zewail, A. H. *Chem. Phys. Lett.* **2006**, *420*, 1–7.
(25) Lin, M. M.; Meinhold, L.; Shorokhov, D.; Zewail, A. H. *Phys. Chem. Chem. Phys.* **2008**, *10*, 4227–4239.

JA808720J